COMMUNICATION

Electronic Supplementary Information

Nickel-selenide templated binary metal-organic frameworks for efficient water oxidation

Suxian Xu,[a] Jian Du,[a] Jiayuan Li,[a] Licheng Sun,[abc] and Fei Li*[a]

---

[a] State Key Laboratory of Fine Chemicals, DUT-KTH Joint Education and Research Centre on Molecular Devices, Dalian University of Technology, Dalian, 116024, China. E-mail: lifei@dlut.edu.cn
[b] Department of Chemistry, KTH Royal Institute of Technology, Stockholm, 10044, Sweden.
[c] Center of Artificial Photosynthesis for Solar Fuels, School of Science, Westlake University, 310024, Hangzhou, China.

Experimental Sections

Chemicals. Iron chloride tetrahydrate ($FeCl_2·4H_2O$, 99.99%), ethylene glycol (EG, 99.99%), terephthalic acid (1,4-H_2BDC, 99%), selenium (Se, 99.99%), and potassium hydroxide (KOH, 95%) were purchased from Aladdin chemical company and used without any further purification. *N,N*-dimethylformamide (DMF), ethanol (CH_5OH), hydrochloric acid (HCl) were analytical pure and obtained from commercial supplier. Ni foam (NF, 2 cm × 1 cm, bulk density 2000 mg/cm^2, thickness 1.5 mm) was purchased from Suzhou jiashide metal foam Co., Ltd.

Preparation of NiSe$_x$/NF electrode. Commercial NF was cut into 1 cm × 2 cm, and was washed successively with 2 M HCl solution and acetone under ultrasonication for 30 min to remove the organic residue and oxide layer of the surface, and the resultant NF was rinsed with ethanol and deionized water, and then dried at room temperature. Firstly, the NiSe$_x$ nanosheets electrode was growth on the NF by a one-step solvothermal process[1]: Se powder (32 mg, 0.4 mmol) was dissolved in a 60 mL homogeneous solution containing 20 mL of EG and 40 mL of ethylenediamine. After continuously stirred for 30 min, the mixture was transferred into 100 mL Teflon-lined stainless steel autoclave and a piece of NF was placed into autoclave titling against the wall at a certain angle, then the autoclave is sealed and continuously heated at 160 °C for 24 h in an oven. After the reaction, the autoclave was cooled down to room temperature, the black electrode was carefully removed from the reaction vessel, and washed alternatively with DMF, ethanol and deionized water, and finally dried at 60 °C for 6 h in a vacuum oven.

Preparation of NiFe-MOF/NiSe$_x$/NF electrode.[2] In order to obtain NiFe-MOF/NiSe$_x$/NF hybrid electrode, the prepared NiSe$_x$/NF was immersed in a 50 mL Teflon-lined stainless steel autoclave with a homogenous solution of

$FeCl_2$•$4H_2O$ (96 mg, 0.48 mmol), 1,4-H_2BDC (80 mg, 0.48 mmol), DMF (14 mL), ethanol (1 mL) and deionized water (1 mL). The autoclave was subsequently sealed and maintained at 125 ^oC for 6 h to allow the growth of NiFe-MOF nanosheets on the $NiSe_x$/NF to form NiFe-MOF/$NiSe_x$/NF hybrid electrode. After cooling down to room temperature, the hybrid electrode was taken out and washed with ethanol and deionized water, followed by drying at 60 ^oC for 6 h in a vacuum oven for further characterization. The catalyst loading of the NiFe-MOF/$NiSe_x$/NF electrode was 2.00±0.02 mg cm^{-2}.

Preparation of NiFe-MOF/NF electrode. The NiFe-MOF/NF electrode was synthesized with the same process, except that the $NiSe_x$/NF electrode was replaced by NF.

Preparation of $NiFe(OH)_y/NiSe_x$/NF electrode. The $NiFe(OH)_y/NiSe_x$/ NF electrode was synthesized with the same process without the 1,4-H_2BDC. The catalyst loading of the $NiFe(OH)_y/NiSe_x$/ NF electrode was 1.38±0.02 mg cm^{-2}.

Preparation of Pt/C/NF electrode. The Pt/C/NF electrode was prepared by dispersing 10 mg Pt/C into 1 mL mixed solution containing 0.45 mL ethanol, 0.5 mL water and 0.05 mL 5% Nafion, the mixture was then ultrasonicated for at least 60 min to form a homogenous ink. Subsequently, 0.2 mL of the suspension was dropped on the acid-treated NF and dried at 60 ℃ to obtain Pt/C/NF as working electrode. The catalyst loading was 2.0 mg cm^{-2}.

Preparation of IrO_2/NF electrode. The IrO2/NF electrode was fabricated with the same process, except that the Pt/C was replaced by IrO_2. The catalyst loading was 2.0 mg cm^{-2}.

Material characterization. The dimension and morphology of as-prepared electrodes were characterized by field emission scanning electron microscopy (FESEM, Nova NanoSEM 450). The lattice fringe and microstructure of the materials were studied by transmission electron microscopy (TEM, FEI TF30) and the elemental mapping of the materials were performed by energy-dispersive X-ray spectroscopy (EDX, FEI TF30). X-ray diffraction (XRD) pattern was acquired on D/max-2400 diffractometer (Japan Rigaku Rotaflex) with Cu Kα radiation (λ = 154.1 Å) to obtain the crystal structure. The element states and composition of the electrode was clarified by X-ray photoelectron spectroscopy (XPS) (Thermo Scientific ESCALAB250). The binding energy (BE) was standardized with respect to the C 1s peak at 284.6 eV. FT-IR spectra (KBr pellets) were acquired with a Thermo Electron NEXUS 6700 FT-IR spectrometer. Raman spectroscopy were collected on a DXR Smart Raman using Ar^+ laser excitation.

Electrochemical measurements. All electrochemical measurements were conducted on a CHI 760E electrochemical workstation (Shanghai Chenhua Instrument Co., Ltd) with a three-electrode system at room temperature. The as-prepared materials as the working electrode, HgO/Hg (1 M KOH) electrode as the reference electrode, and the Pt wire and carbon rod as the counter electrodes, respectively. The electrolyte is 1 $_M$ KOH solution. All the potentials were converted to reversible hydrogen electrode (RHE) scale, $E_{RHE}=E_{HgO/Hg}$ + 0.0592pH + 0.107 V. Before OER and HER tests, each working electrode was activated by continuous cyclic voltammetry (CV) until the curve is invariable. For OER tests, CVs were performed at a scan rate of 5 mV s^{-1} in the potential range of 0.2 to 1.0 V vs HgO/Hg, while for HER measurements, CV data was recorded at a scan rate of 5 mV s^{-1} in the potential range of -0.8 to -1.5 V vs HgO/Hg, all the CV curves are corrected with *iR*-compensation unless specifically stated by the equation: $E = E_0 - iR_s$ (E_0 is the measured potential, R_s is the solution resistance). The Tafel slopes were calculated based on CV (with *iR* drop compensation) and calculated by plotting potential against Log (current density). The electrochemical impedance spectroscopy (EIS) was evaluated at the overpotential of 230 mV at the amplitude of the sinusoidal voltage of 5 mV with a frequency loop from 100 kHz to 0.01Hz. The stability tests were recorded by chronopotentiometry at the current density of 10 mA cm^{-2} without *iR*-compensation.

The electrochemically active surface areas (ECSAs) were evaluated from the electrochemical double-layer capacitance (C_{dl}), the C_{dl} was obtained from CVs measured in a non-Faradaic region at different scan rate (v = 10, 20, 30, 40, 50 and 60 mV s^{-1}) in the potential range of 0.1 to 0.2 V vs HgO/Hg. The current differences at 0.15 V against scan rates were fitted to acquire the C_{dl}, $C_{dl} = I_c / v$, where I_c and v are charging current (mA / cm^2) and scan rate (mV / s).

The Faradaic efficiency (FE) of the electrode was recorded by a home-made single compartment gas-light cell with the as-prepared electrode as the anode and cathode. The cell was bubbling Ar for 30 min for degassing the solution before measurement. The evolved gas was directly collected under the continuous current of 5 mA for 1h and quantified by gas chromatography. FE was finally determined by the comparison of the theoretically calculated gas and experimentally quantified gas.

Supplementary Figure

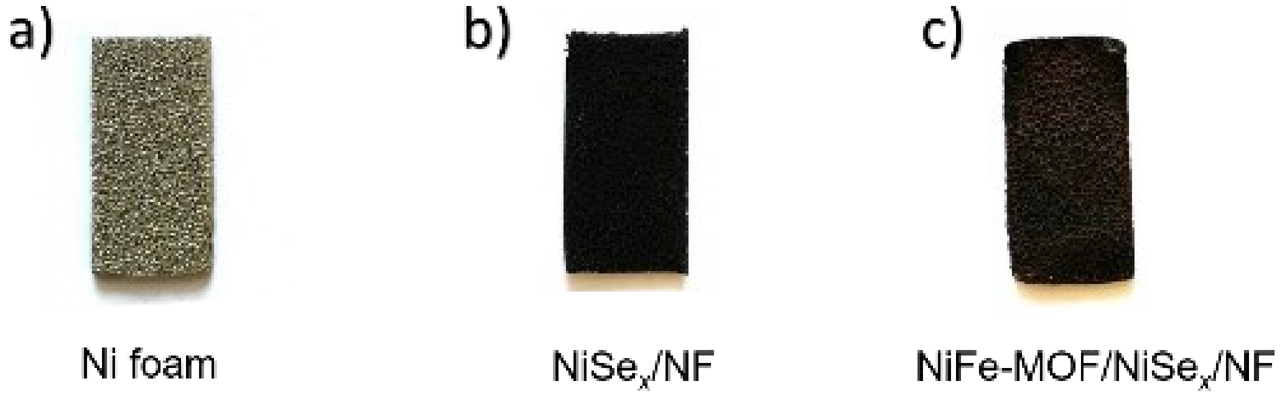

Figure S1. The photograph of a) Ni foam, b) NiSe$_x$/NF, c) NiFe-MOF/ NiSe$_x$/NF.

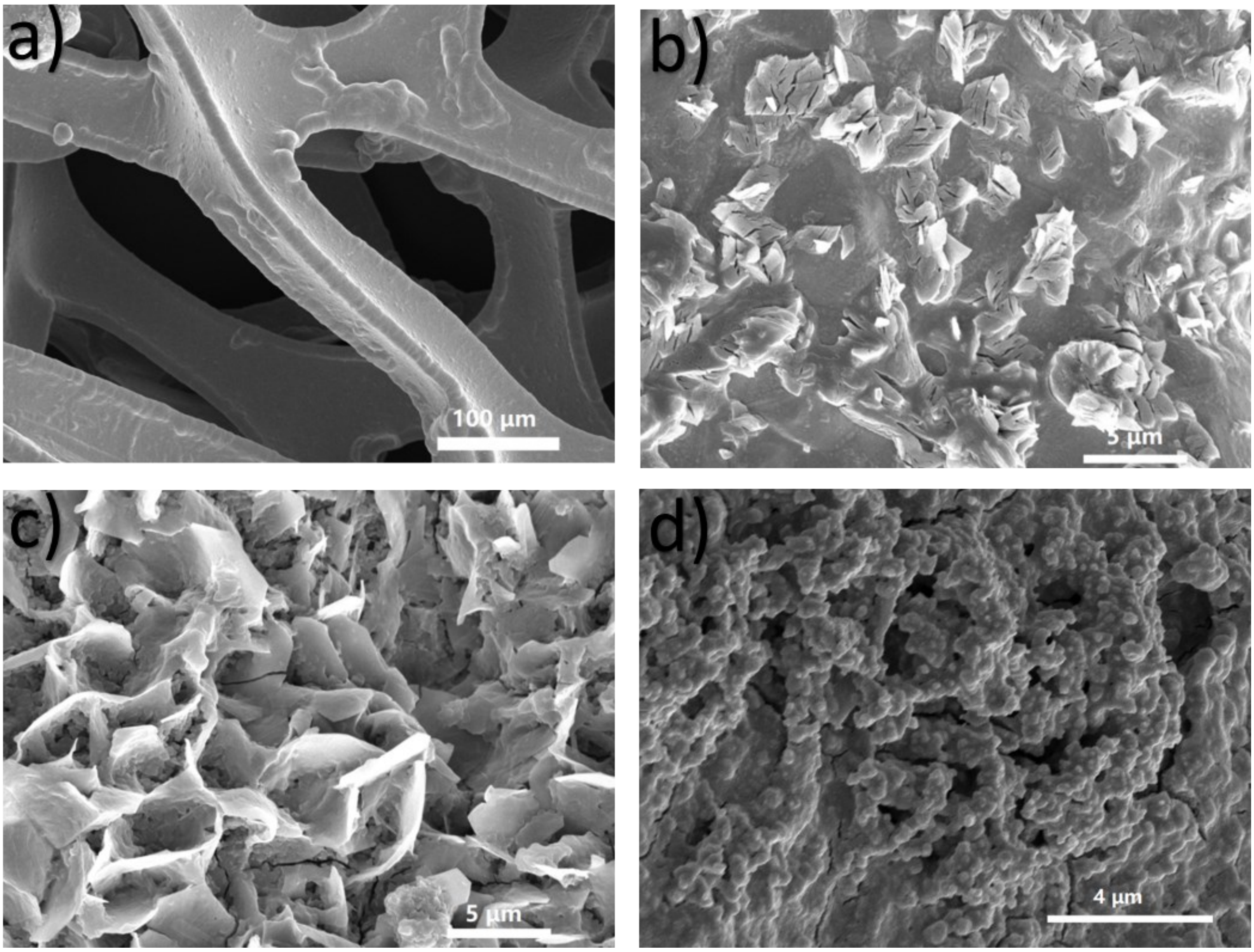

Figure S2. SEM images of a) pristine Ni foam, b) NiFe-MOF/NF, c) $NiSe_x$/NF, and d) $NiFe(OH)_y/NiSe_x$/NF.

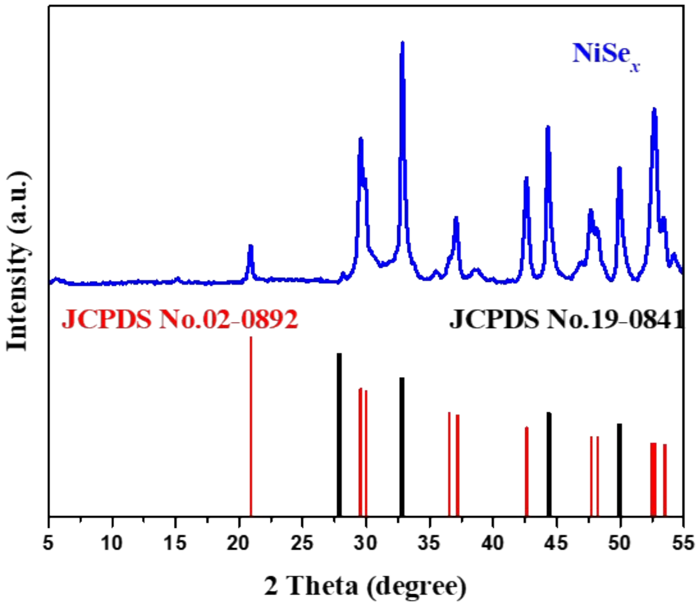

Figure S3. XRD patterns of NiSe$_x$, the NiSe$_x$ were collected by ultra-sonication from NiSe$_x$/NF in ethanol solution.

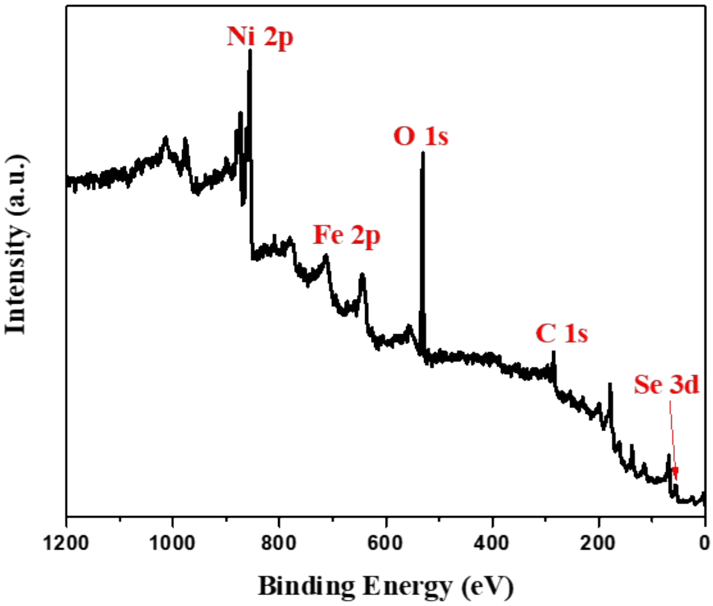

Figure S4. XPS survey spectrum of as-prepared NiFe-MOF/NiSe$_x$/NF.

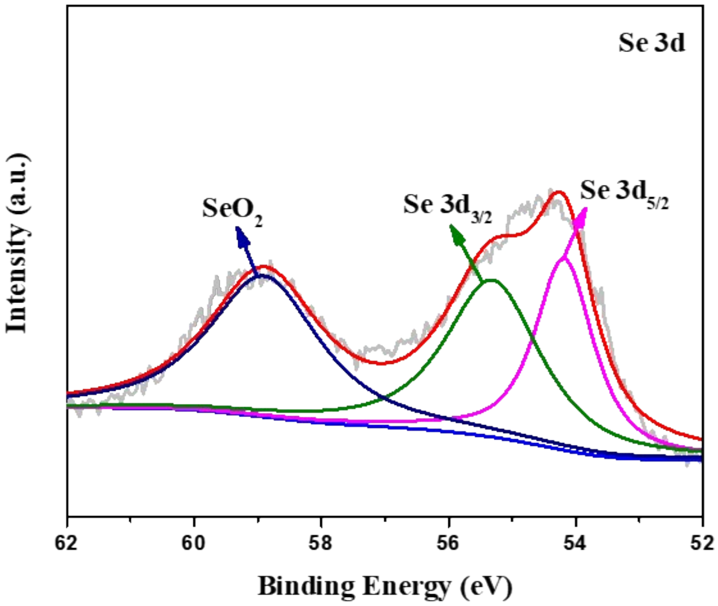

Figure S5. The high-resolution XPS spectra of Se 3d.

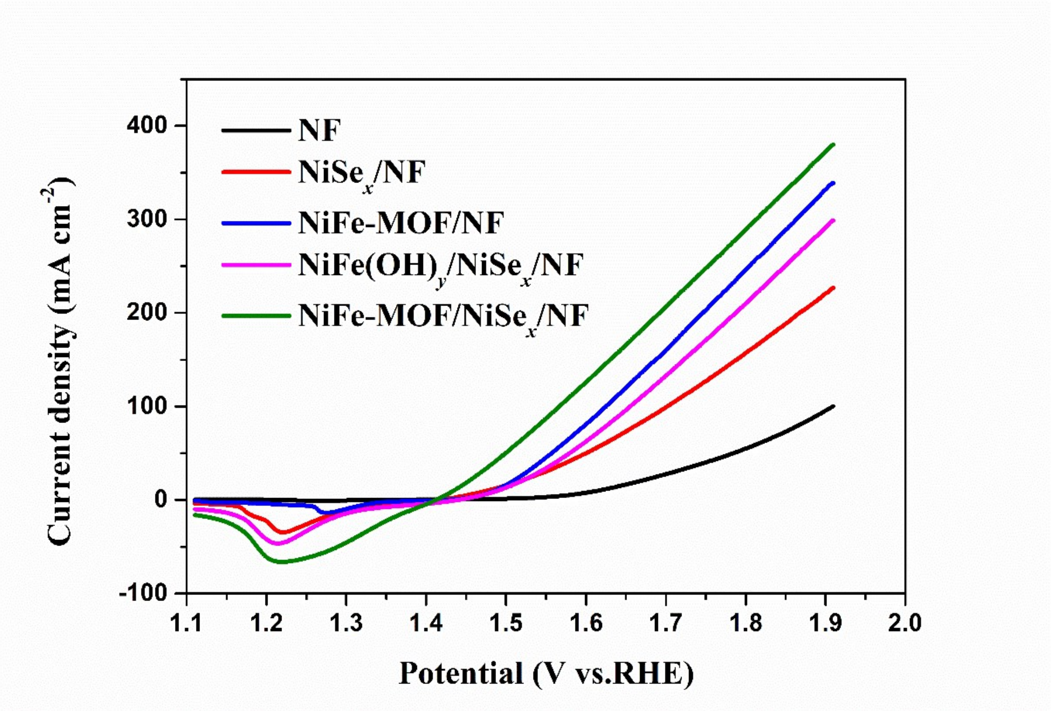

Figure S6. Polarization curves of NiFe-MOF/NiSe$_x$/NF, NiFe(OH)$_y$/NiSe$_x$/NF, NiFe-MOF /NF, NiSe$_x$/NF, and NF toward OER without *iR*-compensation.

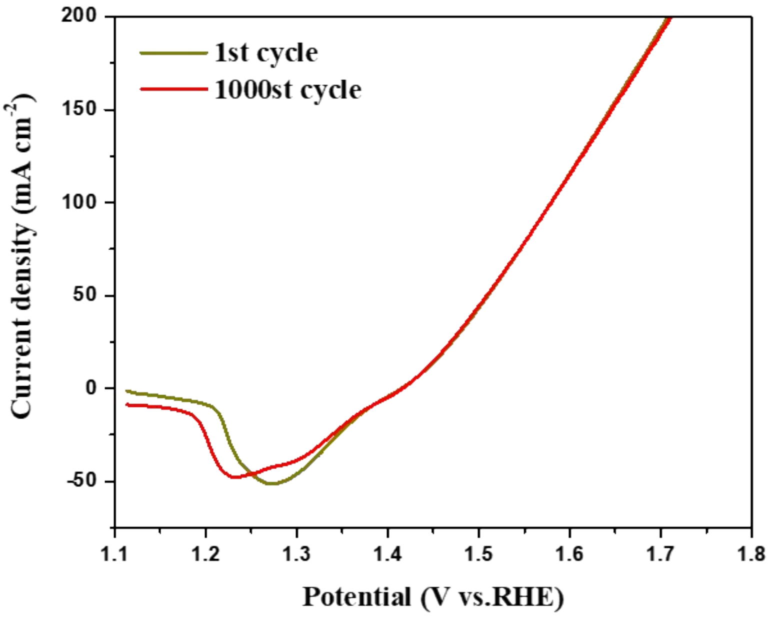

Figure S7. Polarization curves of NiFe-MOF/NiSe$_x$/NF before and after 1000 cycles in 1.0 $_M$ KOH.

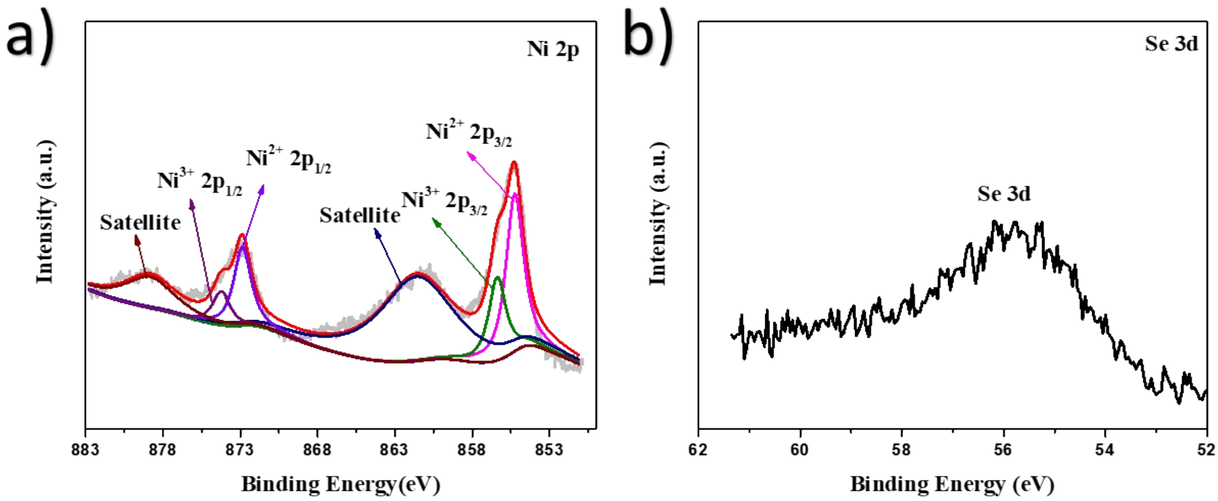

Figure S8. High-resolution XPS spectra of a) Ni 2p and b) Se 3d after OER electrochemical stability test.

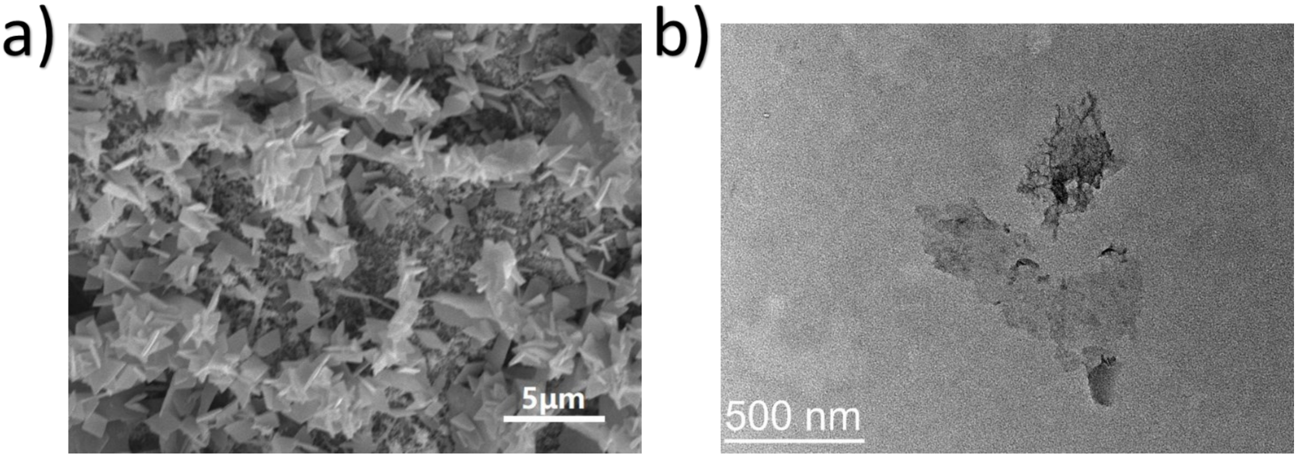

Figure S9. a) SEM and b) TEM image of NiFe-MOF/NiSe$_x$/NF after OER electrochemical test.

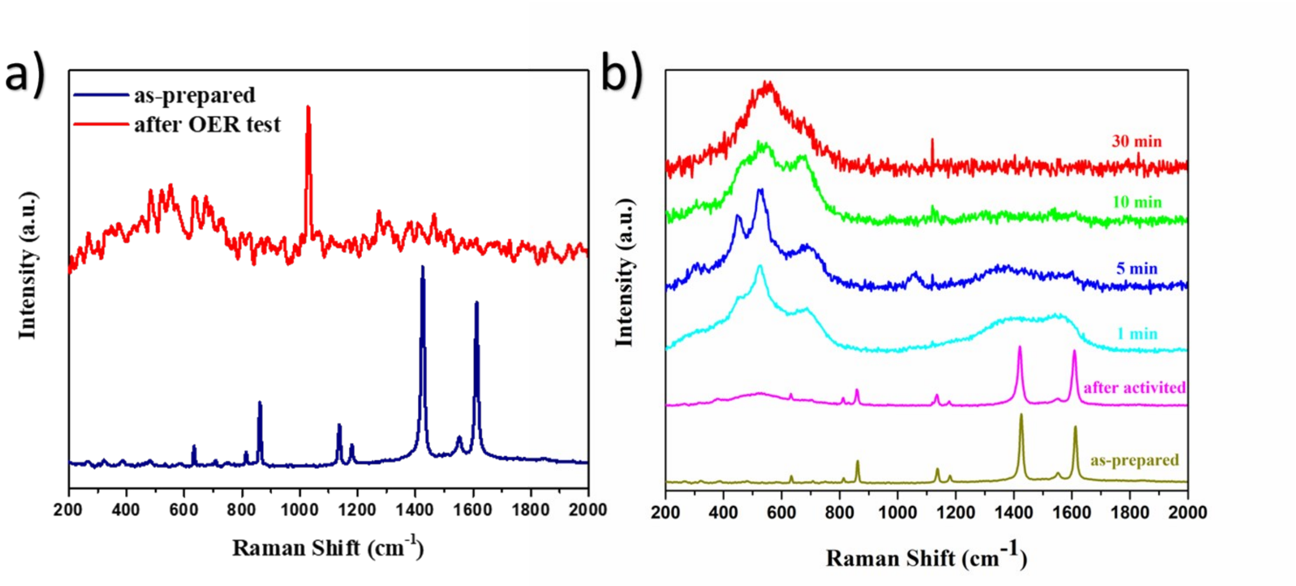

Figure S10. Raman spectra of NiFe-MOF/NiSe$_x$/NF a) before and after OER electrochemical stability test, and b) the changes of Raman spectra during the first 30 min of electrolysis.

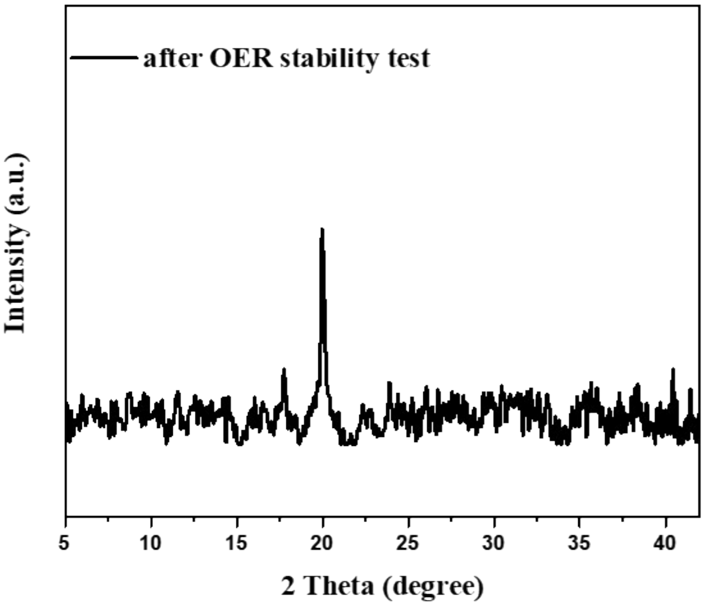

Figure S11. XRD pattern of NiFe-MOF/NiSe$_x$ after OER electrochemical stability test， the NiFe-MOF/NiSe$_x$ were collected by ultra-sonication from NiFe-MOF/NiSe$_x$/NF in ethanol solution.

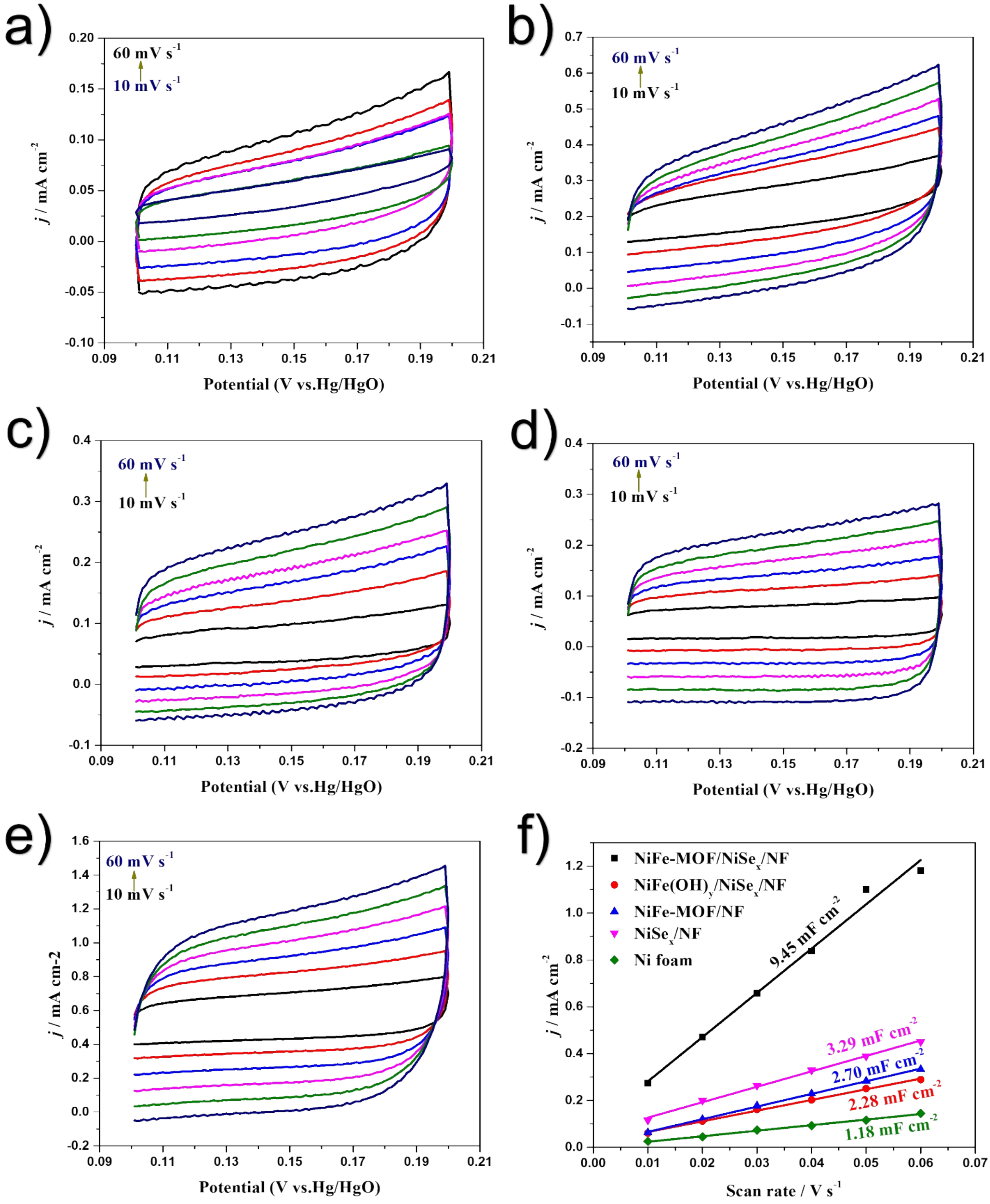

Figure S12. CV curves of a) NF, b) $NiSe_x$/NF, c) $NiFe(OH)_y/NiSe_x$/NF, d) NiFe-MOF/NF and e) NiFe-MOF/$NiSe_x$/NF at various scan rate (10, 20, 30, 40, 50 and 60 mV s^{-1}) in the potential range of 0.1～0.2 V vs HgO/Hg and f) Current densities at 0.15 V vs HgO/Hg as a function of scan rate for NF, $NiSe_x$/NF, $NiFe(OH)_y/NiSe_x$/NF, NiFe-MOF/NF and NiFe-MOF/$NiSe_x$/NF.

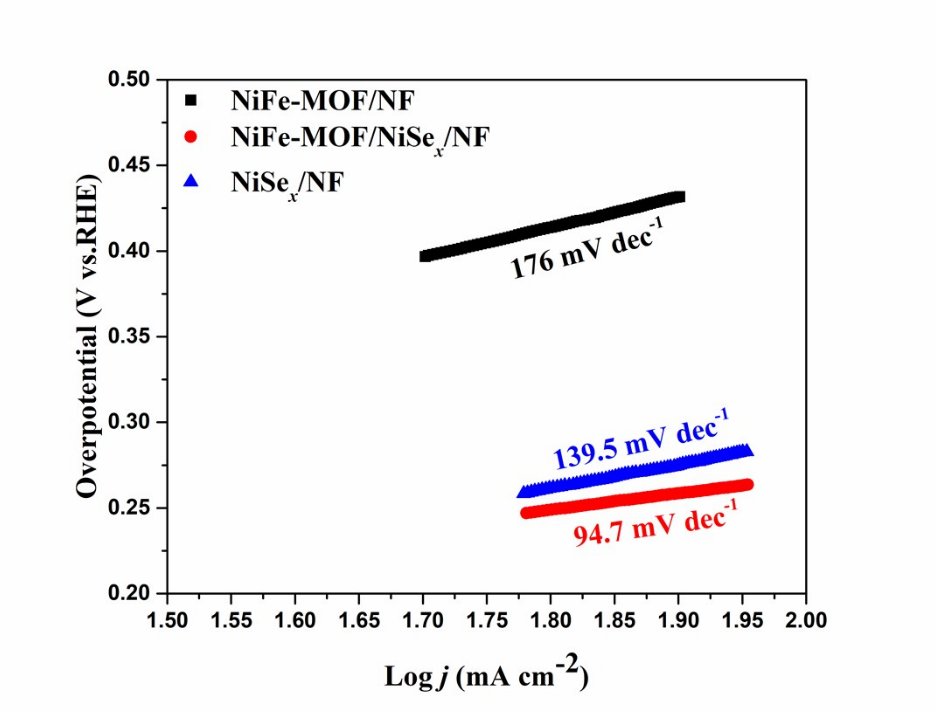

Figure S13. Tafel plots of NiFe-MOF/NF, NiFe-MOF/NiSe$_x$/NF and NiSe$_x$/NF.

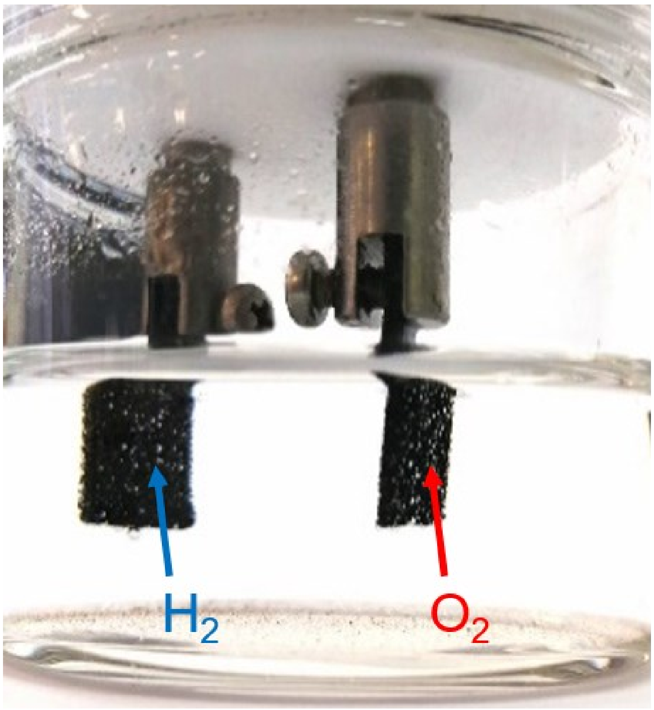

Figure S14. Photograph shows the generation of hydrogen and oxygen bubbles from overall water splitting in cathode and anode in a two-electrode system.

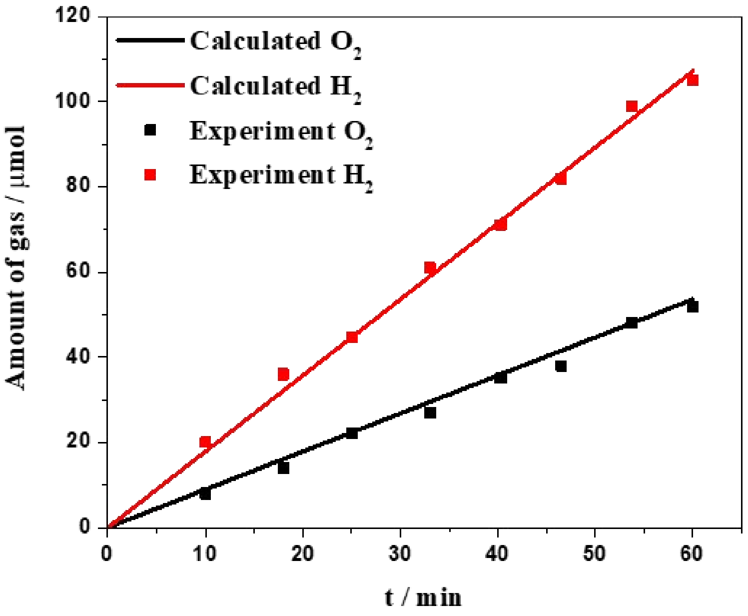

Figure S15. The amount of O_2 and H_2 calculated and experimental measured at the current density of 5 mA cm^{-2} for overall water splitting to determine the Faradaic efficiency.

Table S1 Comparison the electrocatalytic performance of NiFe-MOF/$NiSe_x$/NF for OER with recent reported catalysts.

Catalyst	Substrate	Electrolyte	η(mV)	Tafel slope (mV/dec)	Reference
NiFe-MOF/$NiSe_x$/NF	**NF**	**1.0 M KOH**	**198@10 mA cm^{-2}** **230@10 mA cm^{-2}**	**30.6**	**This work**
NiFe LDH/NF	NF	1.0 M NaOH	240@10 mA cm^{-2}	—	*Science*, **2014**, 345, 1593.
NiFe-MOF/NF	NF	1.0 M KOH	240@10 mA cm^{-2}	34.0	*Nat. Commun*., **2017**, 8, 15341.
MIL-53 (FeNi)/NF	NF	1.0 M KOH	233@50 mA cm^{-2}	31.3	*Adv. Energy Mater.,* **2018**, 8 (21).
NiFe-NFF	NFF	1.0 M KOH	228@10 mA cm^{-2}	38.9	*Adv. Funct. Mater*., **2018**, 29 (6).
NiFe-MOFs NSs	GCE	1.0 M KOH	221@10 mA cm^{-2}	56.0	*Angew. Chem. Int. Ed.*, **2019**, 58 (21).
NiFe-UMNs	GCE	1.0 M KOH	260@10 mA cm^{-2}	30.0	*Nano Energy*, **2018**, 44.
NiCo-UMOFNs	Cu foam	1.0 M KOH	189@10 mA cm^{-2}	42.0	*Nat. Energy*, **2016**, 1, 16181.
Ni-MOF@Fe-MOF	GCE	1.0 M KOH	265@10 mA cm^{-2}	82.0	*Adv. Funct. Mater*., **2018**, 28, 1801554.
$Ni_xFe_{1-x}Se_2$-DO	NF	1.0 M KOH	195@10 mA cm^{-2}	28.0	*Nat. Commun*., **2016**, 7, 12324.
3-D Fe-NiSe NWs	NF	1.0 M KOH	233@10 mA cm^{-2}	48.0	*J. Mater. Chem. A*., **2017**, 5, 14639.
Fe/Ni-BTC	NF	0.1 M KOH	270@10 mA cm^{-2}	47.0	*ACS Appl. Mater. Interface*, **2016**, 8, 16736.

NF: Ni foam, NFF: NiFe foam, GCE: glass carbon electrode.

Table S2 Comparison the electrocatalytic performance of NiFe-MOF/NiSe$_x$/NF for overall water splitting with recent reported bifunctional catalysts.

Catalyst	Electrolyte	Potential (V)	Reference
NiFe-MOF/NiSe$_x$/NF	**1.0 M KOH**	**1.59@10 mA cm^{-2}**	**This work**
NiFe LDH	1.0 M KOH	1.7@10 mA cm^{-2}	*Science*, 2014, 345, 1593.
$NiCo_2O_4$	1.0 M KOH	1.65@10 mA cm^{-2}	*Angew. Chem. Int. Ed.,* **2016**, *55*, 6290.
EG/$Co_{0.85}$Se/NiFe-LDH	1.0 M KOH	1.67@10 mA cm^{-2}	*Energy Environ. Sci.,* **2016**, *9*, 478.
NiFe-MOF/NF	0.1 M KOH	1.55@10 mA cm^{-2}	*Nat. Commun*., **2017**, 8, 15341.
Ni@NC-800	1.0 M KOH	1.6@10 mA cm^{-2}	*Adv. Mater.* **2017**, *29*, 1605957.
CoP/NCNHP	1.0 M KOH	1.64@10 mA cm^{-2}	*J. Am. Chem. Soc.* **2018**, *140*, 2610.
Ni_3Se_2/NF	1.0 M KOH	1.62@10 mA cm^{-2}	*J. Mater. Chem. A*., **2019**, 7, 3344.
NiSe/NF	1.0 M KOH	2.10@10 mA cm^{-2}	*Adv. Energy Mater.,* **2018**, 8, 1702704
$(Ni, Co)_{0.85}Se$	1.0 M KOH	1.65@10 mA cm^{-2}	*J. Mater. Chem. A*., **2018,** 6, 7585
Co_1Mn_1CH	1.0 M KOH	1.68@10 mA cm^{-2}	*J. Am. Chem. Soc.* **2017**, 139, 8320.
CoFe/NF	1.0 M KOH	1.64@10 mA cm^{-2}	*Small* **2018**, 14, 1702568.

NF: Ni foam, GCE: glass carbon electrode.

References

1 J.Zhou, L. Yu, Q. Zhu, C. Huang, Y. Yu, *J. Mater. Chem. A*, 2019, **7**, 18118.

2 F. Sun, G. Wang, Y. Ding, C. Wang, B. Yuan, Y. Lin, *Adv. Energy Mater*., 2018, **8**, 1800584.